

Excited-State Dynamics in the Green Fluorescent Protein Chromophore

Debabrata Mandal,^{‡,§} Tahei Tahara,^{*,‡} and Stephen R. Meech^{*,†}

Molecular Spectroscopy Laboratory, The Institute of Physical and Chemical Research (RIKEN), 2-1 Hirosawa, Wako 351-0198, Japan, and School of Chemical Sciences and Pharmacy, University of East Anglia, Norwich NR4 7TJ, United Kingdom

Received: June 26, 2003; In Final Form: October 24, 2003

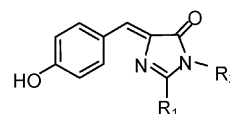
The remarkable suppression of radiationless decay by the green fluorescent protein (GFP) is investigated through ultrafast fluorescence spectroscopy of its isolated chromophore in solution. Decay data are measured by fluorescence up-conversion as a function of solvent and wavelength for both neutral and anionic forms of the chromophore. All fluorescence decays are found to be well described by two exponentially decaying components. The effect of medium viscosity is slight, suggesting that the intramolecular motion promoting radiationless decay is a volume-conserving one. A minor effect of solvent polarity and H-bonding ability on the decay times is observed. The two decay constants are independent of emission wavelength, but their relative weights are not. Time-resolved fluorescence spectroscopy shows that the Stokes shift is complete in <100 fs, and that subsequent spectral evolution is limited to a small spectral narrowing. These data are discussed in terms of a two-state two-mode model, originally proposed to describe isomerization in bacteriorhodopsin (Gonzalez-Luque et al. *Proc. Natl. Acad. Sci. U.S.A.* **2000**, 97, 9379). It is suggested that modification to the displacement and curvature of the excited-state potential energy surface of the chromophore by the protein may be sufficient to account for the dramatic enhancement of chromophore fluorescence in GFP.

1. Introduction

Applications of the green fluorescent protein (GFP) isolated from *Aequorea victoria* as a noninvasive genetically encoded fluorescence marker are widespread and well established.^{1,2} The mechanism of formation of the covalently bound chromophore of GFP involves a cyclization and oxidation reaction among the Ser65, Tyr66, and Gly67 residues to yield the structure shown below (Scheme 1).³ In the folded protein the planar chromophore is located in the center of an 11-stranded β -barrel structure, with some degree of rotational freedom.⁴ The chromophore is covalently bound to the protein backbone and further constrained by hydrogen bonding at the phenolic hydroxyl and carbonyl groups. The photodynamics of the intact protein have been investigated by ultrafast spectroscopy.^{5–7} A proton relay reaction was observed, involving ultrafast excited-state proton transfer from the electronically excited neutral form of the chromophore, to yield a fluorescent anionic state in an unrelaxed configuration. The unrelaxed state may be further stabilized by protein reorganization. This model has been supported and extended by a number of theoretical and experimental studies of GFP and its mutants.^{4,8–10}

In contrast to the rather complete understanding of the photophysics of the intact protein, the observation¹¹ that when the protein is denatured the fluorescence yield of the chromophore decreases by 4 orders of magnitude has yet to be fully explained. An understanding of this remarkably effective protein–chromophore interaction is desirable for a number of

SCHEME 1: Structure of the GFP Chromophore, which Is Attached to the Protein at R₁ and R₂^a



^a In the model compound R₁ = R₂ = CH₃.

reasons. First, at a fundamental level one would like to have a complete grasp of the photophysics of such an important fluorescence marker.

Second, the development of new marker proteins requires an understanding of the photophysical behavior of the chromophore. Two examples may be cited. (a) It is known that some GFP mutants are only very weakly fluorescent, yet the X-ray structure data do not reveal a significant difference in protein packing around the chromophore, which might explain this result.¹² (b) It is now established that in the DsRed fluorescent protein (which has a chromophore of the structure shown above, with the conjugation length extended by substitution of a –C=N–C=O group at R₁¹³) the intense red fluorescence is a property of the tetramer. The protein monomer itself is only weakly fluorescent. However, monomeric fluorescence may be partially restored by random and directed mutagenesis.¹⁴ Further, during maturation of DsRed a weakly fluorescent green emitting chromophore is detected.¹⁵ Evidently the fluorescence enhancing protein–chromophore interaction does not operate in every intact protein in which the chromophore is found. To intervene in a rational manner to optimize mutants of GFP or DsRed for imaging or other purposes presupposes an understanding of the radiationless decay mechanism of the chromophore.

Third, the isolation of proteins containing a GFP-like chromophore is increasingly common.^{16–18} Examples have been

* Address correspondence to these authors. E-mail: tahei@riken.jp (T.T.) and s.meech@uea.ac.uk (S.R.M.).

[‡] The Institute of Physical and Chemical Research (RIKEN).

[§] Current address: Department of Chemistry, Visva-Bharati University, Santiniketan, India.

[†] University of East Anglia.

isolated from coral and sea anemone as well as jellyfish. These proteins may be fluorescent or nonfluorescent, but are often highly colored. In this case photophysical investigations of the kind reported here are important in understanding the physical origin of coloration in biology.

Following the original work of Niwa and co-workers¹¹ a number of groups investigated the photophysics of synthetic analogues of the GFP chromophore. Synthetic models include 4'-hydroxybenzylidene-2,3-dimethylimidazolinone (HBDI, $R_1 = R_2 = \text{CH}_3$) studied here, and 4'-hydroxybenzylidene-2-methylimidazolinone-3-acetate (HBMIA, $R_2 = \text{CO}_2\text{C}_2\text{H}_5$).¹⁹ Niwa and co-workers showed that, like the denatured protein, HBMIA is essentially nonfluorescent in fluid solution. However, in a glass at 77 K the fluorescence recovered to levels comparable to that of the protein. It was also established that the electronic transitions of the chromophore are shifted to lower energy in the protein.¹¹ We measured the ultrafast ground-state recovery dynamics of HBDI at a range of temperatures and viscosities.^{20–23} It was established that the dominant radiationless decay pathway was internal conversion (IC). The rate of IC was found to be only a weak function of solvent viscosity. Separation of viscosity and thermal effects for HBDI (and a related model compound lacking the hydroxyl group) showed that IC is barrierless at room temperature, but exhibits an apparent activation barrier in rigid media.²³ On the basis of these data it was suggested that the coordinate promoting IC must displace only a small solvent volume. One candidate is the concerted twist about the bridging $\text{C}=\text{C}-\text{C}$ bonds ("hula twist") proposed on the basis of quantum chemical calculations by Weber et al.⁸ Two groups have investigated the resonance Raman (RR) spectra of HBDI, and compared them with that of intact GFP.^{24–26} It was found that the same delocalized stretching mode, involving $\text{C}=\text{C}$ and the imidazolinone ring, dominated both spectra. However, the relative intensities of many lower and higher frequency modes were reduced in the protein.²⁴ Schellenberg and Stübner²⁷ investigated low-temperature photochemical hole burning of HBDI. Several similarities with GFP were noted, including the existence of an unrelaxed form of the HBDI anion. Measurements of the ultrafast fluorescence of HBDI and HBMIA have also been reported.^{28,29} As expected from the low quantum yield the excited-state decay times were ultrafast. In addition, non-single-exponential relaxation and a weak dependence on solvent viscosity were observed.

Here we present a detailed examination of the ultrafast fluorescence decay of both neutral and anionic HBDI in a range of solvents. Time-dependent emission spectra are constructed, revealing new details of the excited-state evolution of HBDI. These results are analyzed and used as the basis for a proposed mechanism for the protein–chromophore interaction leading to extreme suppression of radiationless decay in GFP.

2. Experimental Procedures

The HBDI was synthesized and purified as described by Kojima et al.¹⁹ and characterized by mass spectrometry, NMR, and X-ray crystallography. Crystal structures showed that the *cis* isomer had been synthesized, which is the isomer found in GFP. For ultrafast fluorescence measurements the HBDI concentration was adjusted to yield an optical density at the excitation wavelength of ≈ 1 in a 0.5 mm path length cell (equivalent to concentrations of $<10^{-3}$ M). The anion of HBDI was formed by addition of 2 vol % of 1 M KOH to the solution.

The ultrafast fluorescence up-conversion spectrometer has been described in detail elsewhere.³⁰ Essentially fluorescence was excited by the second harmonic frequency of a mode-locked

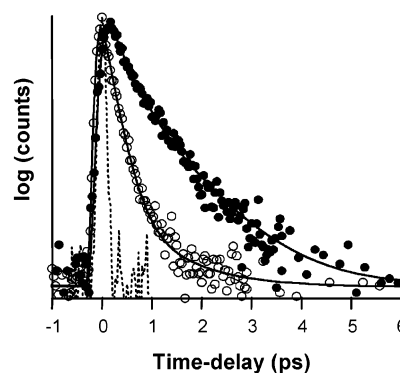


Figure 1. Up-conversion data for HBDI anion (●) and neutral (○) in methanol at 500 nm. The instrument response function (dashed lines) and fits to a sum of two exponential terms are also shown.

titanium sapphire laser. The instantaneous intensity of the resultant fluorescence was measured by up-conversion with the fundamental frequency of the laser in a BBO crystal. The effective time resolution of the present apparatus was measured as 200 fs, from the up-conversion of the instantaneous solvent Raman signal; fluorescence decay times faster than 200 fs can be reliably extracted by deconvolution.³⁰ The power in the excitation beam was attenuated to <3 mW, to minimize thermal effects in the static cell used. Most measurements were made under magic angle conditions, to suppress complicating effects due to solute orientational relaxation. However, fluorescence anisotropy measurements were made in one case, using methods detailed elsewhere.³¹ The excitation wavelengths used were 436 and 380 nm for HBDI anion and neutral, respectively, close to the wavelengths of maximum absorption.

3. Results

The ultrafast fluorescence decay of HBDI and its anion have been measured as a function of emission wavelength and solvent. In almost every case the decay is non-single exponential, as is clearly seen in Figure 1, where the high quality of the data is also apparent. All decay data have been fit to a sum of two exponential components, convoluted with the instrument response function. This provided an excellent fit (also shown in Figure 1).

The results of the analysis at a single wavelength near the peak of the emission spectrum are reported in Table 1. The results for the wavelength dependence are shown in Figure 2.

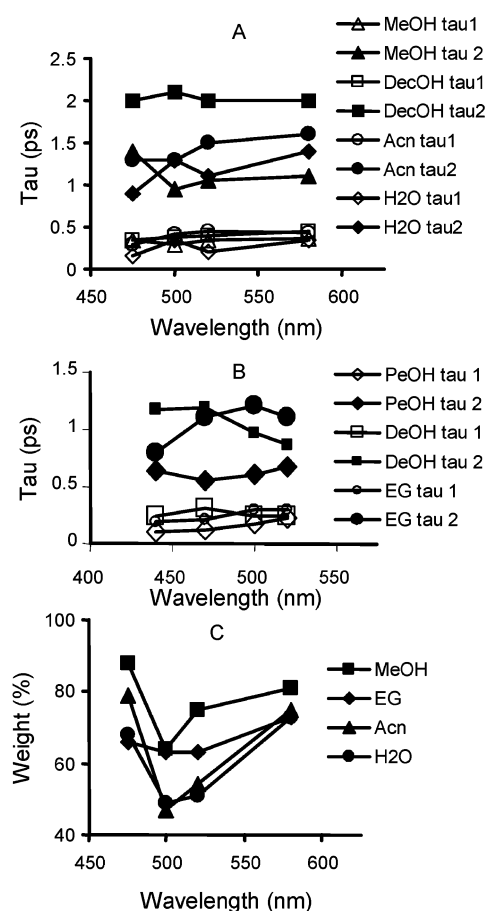
Some conclusions concerning the radiationless relaxation of HBDI may be drawn immediately. First, in all solvents the excited state decay times are independent of wavelength within experimental error. This is shown in Figure 2 for both anion and neutral forms. Importantly, in no case is a rise time observed for either sample, the decay being prompt at all wavelengths. A rise time is expected if the mean frequency of the emission exhibits a time-dependent shift to lower energy. This result constrains the nature of the excited-state dynamics, as discussed in more detail below. Second, in all of the solvents where both forms are readily soluble the decay times for the neutral are shorter than those of the anion, and the weight of the subpicosecond component is more dominant for the neutral form (Table 1).

The solvent dependence of the ultrafast decay is slight for both the neutral and anion forms of HBDI (Table 1). The only significant effect of increasing solvent viscosity is a small increase in the minor, long-lived, component of the decay of the anion. The dominant short component is independent of viscosity within experimental error. Even for the long component

TABLE 1: Decay Constants for HBDI (second row) and Its Anion (first row) as a Function of Solvent

solvent	η/cP	ϵ	τ_1/ps	τ_2/ps
methanol (MeOH)	0.5	32.7	0.34 (0.75) 0.22 (0.93)	1.1 1 ^a
propanol (PrOH)	2.2	20.5	0.37 (0.70) 0.29 (0.91)	1.4 1.5 ^a
pentanol (PeOH)	3.6	13.9	0.37 (0.75) 0.26 (0.84)	1.6 1 ^a
decanol (DeOH)	14.3	7.2	0.39 (0.66) 0.21 (0.84)	2.0 1 ^a
ethyleneglycol (EG)	19.9	37.7	0.46 (0.63) 0.29 (0.69)	3.4 1.2 ^a
water	1	79.8	0.21 (0.51) <0.07 (0.7)	1.1 0.43
acetonitrile (Acn)	0.35	35.9	0.45 (0.54) <i>b</i>	1.4 <i>b</i>
toluene	0.59	2.4	<i>b</i> 0.46 (0.68)	<i>b</i> 1.7 ^a

^a Minor slow component for the neutral has an accuracy of $\pm 40\%$. The normalized weights of the fast component [$a_1/(a_1 + a_2)$], where the a_i are the pre-exponent of the i th component] are given in parentheses. ^b Not measured

**Figure 2.** Wavelength dependence of the decay constants for HBDI extracted from a two-exponential-component analysis: (A) anion, (B) neutral, and (C) the relative weight of the fast component for the anion.

the effect is small; for the alcohol solvents an increase of a factor of 3 in the long decay time of the anion results from a 40-fold increase in solvent viscosity. These data are consistent with earlier observations of ultrafast ground-state recovery times and the temperature dependence of the fluorescence quantum yield.^{20–23} This result is not consistent with radiationless decay arising from an excited-state isomerization along a coordinate displacing a large volume of solvent, such as *cis*–*trans* isomerization about the exo-cyclic double bond of HBDI. Such

intramolecular solute motion would be expected to be sensitive to solvent friction. Other potential relaxation coordinates need to be considered. Indeed complicated fluorescence dynamics (Table 1 and Figure 2) suggest the involvement of more than one coordinate in the relaxation pathway, as discussed further below.

The excited-state decay times of both neutral and anionic forms of HBDI exhibit only a weak dependence on solvent polarity. For example, in the series of *n*-alcohols the polarity varies considerably, but the decay parameters change only slightly (Table 1). The lengthening of the mean lifetime for neutral HBDI in toluene compared to polar protic solvents is the only notable effect of solvent polarity, and suggests that a nonpolar environment can suppress radiationless decay. Table 1 also reveals evidence for an effect of hydrogen bonding on radiationless decay. For example, methanol and acetonitrile have similar polarity and viscosity, yet the HBDI anion has a significantly shorter decay time in the former. Further, for both anionic and neutral forms the excited-state lifetimes are quenched in aqueous solution, the effect being particularly significant for the neutral. Both results suggest a role for hydrogen bonding in the excited-state decay, but neither suggests that H bond formation suppresses radiationless relaxation.

The decay of the fluorescence anisotropy was measured for the HBDI anion in decanol. The initial anisotropy was 0.37, close to the theoretical maximum value of 0.4, expected when absorption and emission transition moments are parallel and aligned with the molecular axis. The anisotropy decay was recorded over 10 ps and did not reveal any unusual features. These results represent strong evidence for the involvement of only a single electronically excited state in absorption and emission. This is consistent with the results of electronic structure calculation.³²

Although the two fluorescence decay times do not vary across the emission spectrum, their relative weights do (Figure 2C). In all solvents studied the weight of the fast fluorescence component for the anion of HBDI is larger at both shorter and longer wavelengths than around the emission maximum. The effect was largest in strongly polar and H-bonding solvents (Figure 2C). This suggests the unusual result of a narrowing of the fluorescence spectrum as a function of time after excitation. This was investigated further for the aqueous solution of the anion (where the effect is largest) by reconstructing time-resolved emission spectra from fluorescence decay profiles, measured at 10 wavelengths spanning the entire emission spectrum. These were analyzed with the two exponential decay constants held fixed at the mean value obtained from free fits to all 10 data sets. This improved the accuracy of the pre-exponents recovered from the fitting. Time-resolved spectra were then reconstructed from the deconvolved fluorescence decays, intensity normalized to the time-integrated fluorescence spectrum. The reconstruction procedure has been described elsewhere.^{33,34} The results are shown in Figure 3. In the first picosecond after excitation the full width at half-maximum height of the fluorescence spectrum decreases by 25% (Figure 3A). The maximum frequency does not change with time, but the spectral narrowing occurs mainly on the high energy side of the spectrum, leading to a very small shift in the mean emission frequency (first moment of the spectrum) with time (Figure 3B). Similar behavior was inferred from measurements on the neutral form of HBDI, although the short lifetime component was more intense on the high energy side than at lower energy.

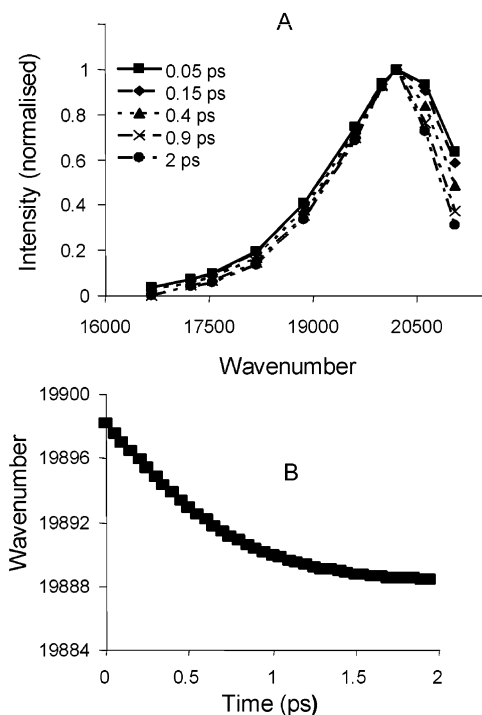


Figure 3. (A) Time-dependent emission spectra for HBDI anion in water. (B) The shift in mean frequency of the spectrum with time.

In summary, the fluorescence decay of the GFP chromophore is observed to be ultrafast, non-single exponential, and hardly sensitive to solvent viscosity or polarity. At no wavelength is a negative amplitude (rise time) observed. This is true for both anionic and neutral forms, although the decay is faster for the latter. The most significant solvent effect is the apparent ability of H-bonding solvent to further quench the excited-state lifetime. The fluorescence decay constants are independent of emission wavelength, but their amplitude varies in a fashion consistent with a time-dependent spectral narrowing. Time-resolved fluorescence spectra revealed a 25% narrowing to occur in 1 ps, accompanied by a negligible shift in the mean emission frequency.

4. Discussion

Although the excited-state decay of HBDI is extremely fast, it is not so fast as to be unprecedented. A number of molecules with some structural affinity to HBDI also exhibit ultrafast internal conversion. Excited-state decay times as short as a few picoseconds have been measured in fluid solvents for triphenylmethane dyes and *cis*-stilbene.^{35,36} In both cases an excited-state isomerization reaction leads to close approach or intersection of ground state and excited state potential energy surfaces, resulting in rapid IC. In both the reaction is believed to be near barrierless (activation energies of <5 kJ mol⁻¹, which exhibit some solvent dependence), as was also found for HBDI in fluid solvents at room temperature.²³ A significant barrier along the reaction coordinate would be expected to result in a considerably longer excited-state decay time.

The isomerization reaction of triphenylmethane dyes is distinguished from that of HBDI by its strong dependence on solvent viscosity.³⁵ In contrast HBDI (like *cis*-stilbene³⁶) exhibits only a very weak dependence on solvent viscosity.^{20–23} The difference between these two classes of barrierless reaction can be understood as a difference in the nature of the isomerization coordinate. For the triphenylmethane dyes the reaction involves the cooperative rotation of three phenyl rings by several

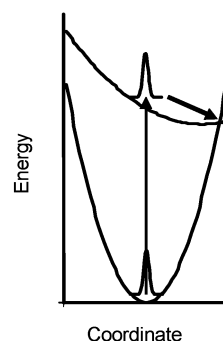


Figure 4. One-dimensional potential energy surfaces for an excited-state isomerization reaction.

degrees.³⁵ Such large-scale intramolecular motion is opposed by solvent friction which may, to a first approximation, be modeled by the solvent viscosity. An explanation for the insensitivity of HBDI (and *cis*-stilbene) excited-state decay times to solvent viscosity is that the isomerization coordinates are volume conserving, i.e. they do not displace a significant solvent volume. In such cases the solvent viscosity is a much less useful measure of the friction experienced by the reaction coordinate. In the case of HBDI one possible volume-conserving coordinate is a concerted rotation about both bridging bonds, followed by a slicing motion of the aromatic rings, the so-called “hula twist”.^{8,37} Electronic structure calculations suggest this as one possibility, although a barrier was predicted along this coordinate for the anion,⁸ which is not observed experimentally.

Although consistent with the present and earlier results, the existence of a volume-conserving pathway to isomerization in HBDI presents a new problem in understanding the role of the protein in promoting chromophore fluorescence in GFP. One plausible and natural explanation for enhanced protein fluorescence is that packing around the chromophore suppresses isomerization about the exocyclic double bond. This is a less obviously plausible explanation when a volume-conserving pathway is available. We will return to this problem below.

As well as the similarity to *cis*-stilbene in solution the excited-state reaction of HBDI has a strong affinity with that of retinal in bacteriorhodopsin (bR): in bR, the fluorescence decay is nonexponential and occurs on a subpicosecond time scale, consistent with a barrierless process, at no wavelength is a fluorescence rise time observed, and the spectral width reportedly narrows slightly with time.³⁸ Further, it has been suggested that the *cis*–*trans* isomerization reaction of retinal in rhodopsin occurs through the hula twist mechanism.³⁹ Thus, some of the calculations and models of excited-state reactions in bR may be useful in interpreting the isomerization reaction of HBDI.

A theoretical treatment of single coordinate barrierless isomerization reactions was given by Bagchi, Fleming, and Oxtoby (BFO).⁴⁰ The essential mechanism is illustrated in Figure 4. The initial, narrow ground-state distribution is transferred to the excited-state surface. The dynamics on the upper surface are determined by the slope of the reactive potential and the friction. Motion on the upper surface is toward sinks, at which the population is efficiently transferred back to the ground state. In the BFO model both local and nonlocal sink functions were considered.⁴⁰ Some of the predictions of the BFO model are consistent with the observations reported above (provided it is accepted that solvent viscosity is not a good model for the friction experienced by the isomerization coordinate, so the predicted reciprocal dependence on viscosity is not expected). In particular the BFO model predicts ultrafast nonexponential fluorescence decays, as observed. However, the feature of the

present data which leads one to rule out the one-dimensional model is the lack of a spectral evolution with time (Figure 3). In the case of motion of the initial population distribution down the excited-state PES toward the sink (where S_1 and S_0 intersect) one expects a red shift in the fluorescence spectrum with time (see Figure 4). In the limit that the excited-state potential surface is flat (as treated by Oster and Nishijima⁴¹) the fluorescence spectrum will not shift, but will broaden with time. Neither of these is observed experimentally. A similar failure to observe any temporal evolution in the stimulated emission spectrum led Hasson et al. to propose a three-state one-dimensional model for the isomerization reaction of bR.⁴² This model, which invokes a coupling of the first and second excited states of retinal, successfully reproduced the main experimental observations of the ultrafast dynamics in bR. However, despite the above-noted similarity between the data for bR and HBDI, a similar mechanism for HBDI is not plausible. Neither fluorescence anisotropy measurements (above) nor electronic structure calculations^{8,32} suggest the presence of a second excited state in the low-energy absorption band.

The model that is most consistent with the ultrafast fluorescence data for HBDI in solution is the two-state two-coordinate model described by González-Luque et al.⁴³ This was proposed as an explanation for ultrafast relaxation in bR. The essential dynamics of the model are displayed in Figure 5A. The initial motion away from the Franck–Condon excited state is along a stretching coordinate that is not strongly coupled to the reactive isomerization coordinate. This process, which may be very fast (<100 fs) depending on the frequency of the mode, accounts for the absence of a fluorescence rise time and the appearance of the instantaneous Stokes loss. At the stationary point reached along the stretching coordinate, from which the sink to S_0 is accessible, intramolecular vibrational energy redistribution (IVR) into low-frequency vibrational and torsional modes of the chromophore takes place. We propose that the spectral narrowing observed occurs as the broad distribution of low-frequency modes initially populated relaxes along the reactive coordinate (Figure 5A). While the IVR proceeds, the motion along the reactive isomerization coordinate occurs, toward the sink where internal conversion to the ground electronic state takes place.

The two-state two-coordinate model is consistent with the time scale of the fluorescence decay of HBDI, its nonexponential nature, and the observed spectral evolution as a function of time. It is also possible to think of the faster decay of the neutral compared to the anion as arising from a different shape of the reactive potential surface. For example, in the anion the sink may be located higher in energy than the stationary point (as in Figure 5), while in the neutral the isomerization coordinate may be energetically downhill. Thus in the neutral subpicosecond vibrational redistribution would dominate, and the second component would be faster than in the anion, as observed (Table 1 and Figure 1).

Thus equipped with a model for the excited-state dynamics of HBDI in solution, it is possible to consider the dramatic effect of the protein matrix in suppressing radiationless decay. The most obvious explanation, that friction arising from packing of the protein matrix about the chromophore opposes motion along the isomerization coordinate, is not consistent with the data. In particular the observations that the isomerization coordinate is a volume-conserving one and that some nonfluorescent GFP mutants have compact structures around the chromophore are both inconsistent with a model in which protein matrix friction enhances the fluorescence. Indeed recent molecular dynamics calculations suggest that there is sufficient rotational freedom

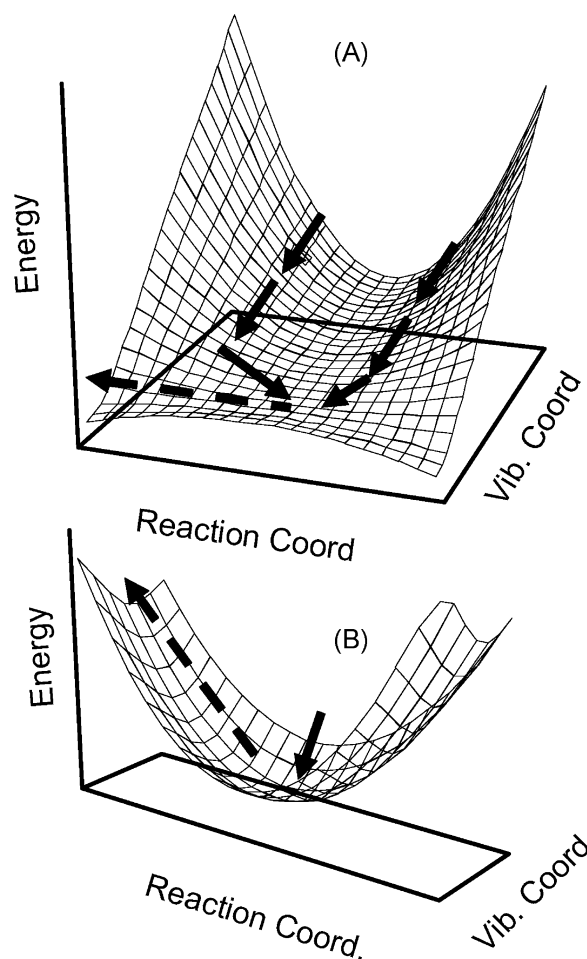


Figure 5. (A) Excited-state PES for the two-state two-mode model. Arrows indicate ultrafast motion along the high-frequency vibrational coordinate to the reactive region of the PES, followed by IVR and relaxation along the reaction coordinate. (B) A possible excited-state two-mode model PES for GFP. The displacement along the stretching coordinate is reduced and the curvature of the reactive surface increased by chromophore–protein interactions.

for the chromophore to undergo a volume-conserving intramolecular reorganization in the protein.⁴

The two-state two-coordinate model⁴³ outlined above allows two new possibilities for the intervention of the protein matrix to suppress the isomerization reaction. First, in GFP the initial relaxation out of the Franck–Condon region may direct the chromophore away from the stationary point from which isomerization occurs, such that the chromophore never accesses the reactive part of the PES. This possibility could be investigated further by resonance Raman (RR) and RR excitation spectra. The available data^{24–26} show that the delocalized stretching coordinate observed around 1560 cm^{-1} is the strongest mode in both HBDI and wtGFP. However, it was also reported that a number of lower frequency modes that are significant in the RR spectra of HBDI and its anion are suppressed in the protein.^{24,25,44} This certainly suggests that the protein may modify the primary coordinate in a two-coordinate model. More detailed RR excitation spectra are required to develop this model further.

The protein may also influence radiationless decay by a modification of the shape of the reactive PES leading to the S_0 – S_1 intersection. The large red shift in the HBDI absorption spectrum between solution and intact protein^{11,22} suggests that the equilibrium position of the excited state is significantly shifted and/or stabilized by the protein matrix. It has not proved

possible to reproduce this large red shift for HBDI in any solvent we have investigated.⁴⁵ A shift in the equilibrium geometry of the excited-state PES such that it is closer to that of the ground state is consistent with the observation that the Stokes loss (for the anionic form of the chromophore) is small in wtGFP. A reduced displacement for the excited state may also be consistent with the simpler RR spectrum of wtGFP relative to HBDI.²⁴ However, it seems unlikely that a simple shift in the potential minimum can be sufficient to account for the complete suppression of such a rapid barrierless radiationless decay. It is also likely that the curvature along the reactive coordinate is increased in the protein, with the result that the barrier between the stationary point and the intersection with the ground state surface is increased. These two effects of protein on the potential energy surfaces are illustrated in Figure 5B. While such model PESs are helpful in rationalizing the data presented, they are necessarily speculative. A more detailed picture of the excited-state dynamics in GFP is only likely to be attained from the kind of detailed quantum mechanical–molecular mechanical calculations that have proved so valuable in interpreting the dynamics of bR.^{43,46} Such calculations, which are beginning to appear,^{8,47–49} (including a two-mode model⁴⁹) will certainly be needed to investigate specific H-bonding between chromophore and protein, and the interaction between the charge distribution in the protein and that of the excited state. Both factors may contribute to the modifications of the PES alluded to above. In this connection it is interesting to note that, while the HBDI form of the chromophore (Scheme 1) has a quantum yield near unity in GFP, a blue fluorescent mutant (tyr66phe) lacking the phenolic hydroxyl group has a much lower yield. In contrast the two corresponding model compounds have very similar photophysical properties in solution.²³ This certainly suggests a role for protein–chromophore hydrogen bond formation in controlling the fluorescence yield, as well as in the proton relay reaction.

The seemingly large spectral shift between solution-phase HBDI and the chromophore in the protein is in contrast to the observed similarity between the gas-phase absorption spectrum of the HBDI anion and the protein.^{50,51} This can be interpreted as the protein structure simply shielding the chromophore from interactions with its surroundings, yielding a similar transition frequency to the gas phase.⁵⁰ However, this conclusion is not obviously consistent with the structural data, which suggest a compact environment for the chromophore, with extensive H-bonding interactions between it and the protein backbone. Another possibility is that a mixture of blue and red shifting intermolecular interactions yields a fortuitous agreement between protein and gas-phase transition energies. Alternatively, it is plausible that the HBDI chromophore in solution adopts a different, blue-shifted, ground-state conformation to that in the gas phase, but H-bonding interactions and the restricted space of the protein lock the chromophore in its red-shifted gas-phase geometry.

It is interesting to close the discussion by noting that the previously close analogy between HBDI and bR becomes a matter of contrast when the role of the protein is considered. In bR the protein accelerates radiationless decay by at least an order of magnitude, while in GFP it suppresses it by at least 3 orders of magnitude. In some senses this divergence is not unexpected: the function of bR is to drive structural change through cis–trans isomerization, while the point of GFP is to emit photons. Nevertheless, these contrasting effects of protein matrix on what are in many respects analogous photophysical processes

are a testament to the rich and diverse range of protein–chromophore interactions.

5. Conclusion

The ultrafast fluorescence of the HBDI chromophore of GFP has been studied in detail as a function of solvent and emission wavelength. The decay of the excited state, which occurs through IC, is non-single exponential, with subpicosecond and picosecond components. The neutral form of the chromophore decays more rapidly than the anionic form. The decay times are remarkably independent of solvent viscosity and polarity. The decay times are also independent of wavelength, but their relative weights are not. The time-dependent fluorescence spectrum has been measured in aqueous solution, and a significant spectral narrowing with a negligible shift in the mean frequency takes place over the first picosecond.

Different representations of the excited-state dynamics have been considered. The model most consistent with all the data on HBDI is a two-state two-mode model, initially proposed to describe ultrafast isomerization in bR.⁴⁰ The mechanism involves evolution along a vibrational coordinate, and subsequent intramolecular vibrational redistribution, and motion along the reactive coordinate leading to IC. The most attractive features of this model are that it is consistent with the available data, and it provides a plausible mechanism for the protein–chromophore interaction leading to the suppression of radiationless decay in wtGFP. It is proposed that the protein modifies both the displacement of low-frequency modes and the curvature of the reactive potential energy surface.

Acknowledgment. S.R.M. would like to thank the Tahara group for their hospitality. S.R.M. thanks JSPS for the award of a visiting fellowship, and D.M. thanks JSPS for a postdoctoral fellowship. Support in the UK from BBSRC and EPSRC is gratefully acknowledged.

References and Notes

- (1) Tsien, R. Y. *Annu. Rev. Biochem.* **1998**, *67*, 509.
- (2) Prendergast, F. G. *Methods Cell Biol.* **1999**, *58*, 1.
- (3) Reid, B. G.; Flynn, G. C. *Biochemistry* **1997**, *36*, 6786.
- (4) Chen, M. C.; Lambert, C. R.; Ugritis, J. D.; Zimmer, M. *Chem. Phys.* **2001**, *270*, 157.
- (5) Chatteraj, M.; King, B. A.; Bublitz, G. U.; Boxer, S. G. *Proc. Natl. Acad. Sci. U.S.A.* **1996**, *93*, 8362.
- (6) Lossau, H.; Kummer, A.; Heinecke, R.; Pöllinger-Dammer, F.; Kompa, C.; Bieser, G.; Jonsson, T.; Silva, C. M.; Yang, M. M.; Youvan, D. C.; Michel-Beyerle, M. E. *Chem. Phys.* **1996**, *213*, 1.
- (7) Winkler, K.; Lindner, J.; Subramaniam, V.; Jovin, T. M.; Vöhringer, P.; *Phys. Chem. Chem. Phys.* **2002**, *4*, 1072.
- (8) Weber, W.; Helms, V.; McCammon, J. A.; Langhoff, P. W. *Proc. Natl. Acad. Sci. U.S.A.* **1999**, *96*, 6177.
- (9) Seebacher, C.; Deeg, F. W.; Bräuchle, C.; Wiehler, J.; Steipe, B. *J. Phys. Chem. B* **1999**, *103*, 7728.
- (10) Brejc, K.; Sixma, T. K.; Kitts, P. A.; Kain, S. R.; Tsien, R. Y.; Ormö, M.; Remington, S. J. *Proc. Natl. Acad. Sci. U.S.A.* **1997**, *94*, 2306.
- (11) Niwa, H.; Ionuye, S.; Horano, T.; Matsuno, T.; Kojima, S.; Kubota, M.; Ohashi, M.; Tsuji, F. I. *Proc. Natl. Acad. Sci. U.S.A.* **1996**, *93*, 13617.
- (12) Kummer, A. D.; Wiehler, J.; Rehder, H.; Kompa, K.; Steipe, B.; Michel-Beyerle, M. E. *J. Phys. Chem. B* **2000**, *104*, 4791.
- (13) Gross, L. A.; Baird, G. S.; Hoffman, R. C.; Baldrige, K. K.; Tsien, R. Y. *Proc. Natl. Acad. Sci. U.S.A.* **2000**, *97*, 11990.
- (14) Cambell, R. E.; Tour, O.; Palmer, A. E.; Steinbach, P. A.; Baird, G. S.; Zacharias, D. A.; Tsien, R. Y. *Proc. Natl. Acad. Sci. U.S.A.* **2002**, *99*, 7877.
- (15) Cotlet, M.; Hofkens, J.; Habuchi, S.; Dirix, G.; van Guyse, M.; Michiels, J.; Vanderleyden, J.; de Schryver, F. C. *Proc. Natl. Acad. Sci. U.S.A.* **2001**, *98*, 14398.
- (16) Lukyanov, K. A.; Fradkov, A. F.; Gueskaya, N. G.; Matz, M. V.; Labas, Y. A.; Savitsky, A. P.; Markelov, M. L.; Zaisky, A. G.; Zhao, X.; Fang, Y.; Tan, W.; Lukyanov, S. A. *J. Biol. Chem.* **2000**, *275*, 25879.
- (17) Martynov, V. I.; Savitsky, A. P.; Martynova, N. Y.; Savitsky, P. A.; Lukyanov, K. A.; Lukyanov, S. A. *J. Biol. Chem.* **2001**, *276*, 21012.

- (18) Prescott, M.; Ling, M.; Beddoe, T.; Oakley, A. J.; Dove, S.; Hoegh-Guldberg, O.; Devenish, R. J.; Rossjohn, J. *Structure* **2003**, *11*, 275.
- (19) Kojima, S.; Ohkawa, H.; Hirano, T.; Maki, S.; Niwa, H.; Ohashi, M.; Inouye, S.; Tsuji, F. I. *Tetrahedron Lett.* **1998**, *39*, 5239.
- (20) Webber, N. M.; Litvinenko, K. L.; Meech, S. R. *J. Phys. Chem. B* **2001**, *105*, 8036.
- (21) Litvinenko, K. L.; Webber, N. M.; Meech, S. R. *Chem. Phys. Lett.* **2001**, *346*, 47.
- (22) Litvinenko, K. L.; Webber, N. M.; Meech, S. R. *Bull. Chem. Soc. Jpn.* **2002**, *75*, 1065.
- (23) Litvinenko, K. L.; Webber, N. M.; Meech, S. R. *J. Phys. Chem. A* **2003**, *107*, 2616.
- (24) Schellenberg, P.; Johnson, E.; Esposito, A. P.; Reid, P. J.; Parson, W. W. *J. Phys. Chem. B* **2001**, *105*, 5316.
- (25) He, X.; Bell, A. F.; Tonge, P. J. *J. Phys. Chem. B* **2002**, *106*, 6056.
- (26) Bell, A. F.; He, X.; Wachter, R. M.; Tinge, P. J. *Biochemistry* **2000**, *39*, 4423.
- (27) Stübner, M.; Schellenberg, P. *J. Phys. Chem. A* **2003**, *107*, 1246.
- (28) Mandal, D.; Tahara, T.; Webber, N. M.; Meech, S. R. *Chem. Phys. Lett.* **2002**, *358*, 495.
- (29) Kummer, A. D.; Kompa, C.; Niwa, H.; Hirano, T.; Kojima, S.; Michel-Beyerle, M.-E. *J. Phys. Chem. B* **2002**, *106*, 7554.
- (30) Takeuchi, S.; Tahara, T. *J. Phys. Chem. A* **1997**, *101*, 3052.
- (31) Takeuchi, S.; Tahara, T. *J. Phys. Chem. A* **1998**, *102*, 7740.
- (32) Voityuk, A. A.; Kummer, A. D.; Michel-Beyerle, M.-E.; Rösch, N. *Chem. Phys.* **2001**, *269*, 83.
- (33) Meech, S. R.; O'Connor, D. V.; Roberts, A. J.; Phillips, D. *Photochem. Photobiol.* **1981**, *33*, 159.
- (34) Maroncelli, M.; Fleming, G. R. *J. Chem. Phys.* **1987**, *86*, 6221.
- (35) Ben-Amotz, D.; Harris, C. B. *J. Chem. Phys.* **1987**, *86*, 4856.
- (36) Todd, D. C.; Fleming, G. R. *J. Chem. Phys.* **1993**, *98*, 269.
- (37) Liu, R. S. H.; Hammond, G. S. *Proc. Natl. Acad. Sci. U.S.A.* **2000**, *97*, 11153.
- (38) Du, M.; Fleming, G. R. *Biophys. Chem.* **1993**, *48*, 101.
- (39) Liu, R. S. H.; Asato, A. E. *Proc. Natl. Acad. Sci. U.S.A.* **1985**, *82*, 259.
- (40) Bagchi, B.; Fleming, G. R.; Oxtoby, D. W. *J. Chem. Phys.* **1983**, *78*, 7375.
- (41) Oster, G.; Nishijima, Y. *J. Am. Chem. Soc.* **1956**, *78*, 1581.
- (42) Hasson, K. C.; Gai, F.; Anfinrud, P. A. *Proc. Natl. Acad. Sci. U.S.A.* **1996**, *93*, 15124.
- (43) González-Luque, R.; Garavelli, M.; Bernardi, F.; Merchán, M.; Robb, M. A.; Olivucci, M. *Proc. Natl. Acad. Sci. U.S.A.* **2000**, *97*, 9379.
- (44) Tozzini, V.; Bizzari, A. R.; Pellegrini, V.; Nifosi, R.; Giannozzi, P.; Iuliano, A.; Cannistraro, S.; Beltram, F. *Chem. Phys.* **2003**, *287*, 33.
- (45) Webber, N. M. Ph.D. Dissertation, 2002, University of East Anglia, UK.
- (46) Warshel, A.; Chu, Z. T. *J. Phys. Chem. B* **2001**, *105*, 9857–9871.
- (47) Toniolo, A.; Granucci, G.; Martinez, T. J. *J. Phys. Chem. A* **2003**, *107*, 3822.
- (48) Das, A. K.; Hasegawa, J. Y.; Miyahara, T.; Ehara, M.; Najatsuji, H. *J. Comput. Chem.* **2003**, *24*, 1421.
- (49) Navarro, E. M.; Negri, F.; Olivucci, M. Private communication.
- (50) Nielsen, S. B.; Lapiere, A.; Andersen, J. U.; Pedersen, U. V.; Tomita, S.; Anderson, L. H. *Phys. Rev. Lett.* **2001**, *87*, 228102.
- (51) Andersen, L. H.; Lapiere, A.; Nielsen, S. B.; Nielsen, I. B.; Pedersen, S. U.; Pedersen, U. V.; Tomita, S. *Eur. Phys. J. D* **2002**, *20*, 597.